Journal of Clinical & Experimental Ophthalmology

Tan et al., J Clin Exp Ophthalmol 2013, 4:5
DOI: 10.4172/2155-9570.1000303

Case Report Open Access

Ocular Phenotypes and *In Vivo* Laser Confocal Microscopy Findings in a Family with Schnyder Corneal Dystrophy Shared the Same *UBIAD1* Mutation Locus (N102S)

Jian-wen Tan, Chao-ran Zhang* and Fei-fei Huang

Department of Ophthalmology, Eye Ear Nose and Throat Hospital of Fudan University, Shanghai 200031, China

Abstract

Purpose: This study aims to observe the ocular phenotypes of a family with Schnyder corneal dystrophy (SCD) and to assess the image features of SCD by in vivo laser corneal confocal microscopy (IVCM).

Methods: A family with SCD was collected, and the corneal lesion of five affected members was observed. Bilateral corneas were examined using IVCM (Heidelberg Retina Tomograph III with Cornea Module) in three adult patients with SCD. Blood samples were collected for genetic analysis in the available family members.

Results: Phenotype heterogeneity was found in five affected individuals with a same mutation (N102S). Slit-lamp examination suggested no crystal in the right eye of a 40-year-old male SCD patient, but crystalline materials were found by IVCM. In some images of IVCM, crack-like striaes and crystalline materials with various shapes were observed in the stroma.

Conclusions: Extremely varied phenotypes between individual patients are demonstrated in this SCD family with a same mutation locus. Slit-lamp examination cannot find mini crystalline deposits in SCD cornea. Crystalline accumulations can be detected by ICVM at the cellular level prior to slit-lamp examination.

Keywords: Schnyder corneal dystrophy; Corneal dystrophy; *In vivo* laser confocal microscopy; Confocal microscopy; *UBIAD1* gene

Introduction

Schnyder corneal dystrophy (SCD) is a rare, autosomal dominant inherited corneal disorder with high penetrance that affects the central and peripheral cornea and is characterized by cholesterol and phospholipid deposition. Those depositions are mainly localized in the corneal epithelium and stroma, and in some cases, the endothelium is involved leading to progressive corneal opacity [1,2]. Corneal crystals which are present only in 54% of SCD patients can facilitate the disease diagnosis [3]. This report documented a Chinese SCD family and further clarified its ocular phenotypes. In this study, we also clarified image features of SCD by IVCM.

Methods

After informed consent, five affected individuals from a Chinese SCD family were examined and their clinical features were recorded. Three adults among them also received IVCM examination. SCD diagnosis was based on clinical manifestations and genotype analysis of *UBIAD1* gene.

In vivo corneal confocal microscopy examination

IVCM [Heidelberg Retina Tomograph III with Cornea Module (HRT III/CM)] was performed on three affected individuals with SCD. Longitudinal resolution of HRT III/CM is 1 μm. A 670 nm diode laser as the light source was applied in HRT III/CM. Before the examination, one drop of topical anesthesia of 0.5% proparacaine hydrochloride (Alcaine, Alcon) was instilled in both eyes. After applying a large drop of contact gel (Berlin, Germany Subsidiary of Bausch and Lomb) on the front surface of the microscope lens. Then, the cornea was accurately examined layer by layer using IVCM.

Genetic analysis

After obtaining informed consent, blood samples were collected (5 ml of blood in EDTA) from the available family members for a molecular genetic analysis. We extracted genomic DNA from peripheral blood leukocytes according to standard procedures. Exons 1 and 2 of *UBIAD1* were amplified by polymerase chain reaction (PCR) using a 25 μl reaction mixture, containing 10× PCR buffer solution (2.5 μl), 2.5 mM dNTPs mixture (2 μl), 50 mM $MgCl_2$ (0.75 μl), forward (5 μM) and reverse (5 μM) primers (1 μl each), Platinum® *Taq* polymerase (0.2 μl) obtained from Invitrogen Biotechnology Co. Ltd (Shanghai, China), sterile distilled water (16.55 μl) and DNA template (1 μl). Primers for the two coding exons of *UBIAD1*: 1F-CTC GTG GGG TGT AAG ACC CAC TT, 1R-GCG GCT TAA ATT AGA AAG CCA CCT; 2F-AGT GCC CAC CTG CAC AGT CTA AG, 2R-CAA ACT GGG CAG CTC CTT TAC AA. The target DNA regions were amplified with the following PCR settings: initial 5 min denaturation step at 94°C and a final 5 min extension step at 72°C with an intervening 30 cycles of 30 s denaturation at 94°C, 30 s annealing at 55°C and 30 s extension at 72°C; the samples were maintained at 4°C until use (PCR Amplifier using ABi9700). Amplicons were evaluated using agarose gels and then sequenced on a 3730XL DNA Analyzer.

Results

Clinical features of SCD

Five affected individuals with SCD were confirmed in a three-

***Corresponding author:** Chao-ran Zhang, Department of Ophthalmology, Eye Ear Nose and Throat Hospital of Fudan University, Shanghai 200031, China, Tel: 64377134 transfer to 803; Fax: 0086-21-64377151; E-mail: 285659395@qq.com

Received August 24, 2013; **Accepted** October 31, 2013; **Published** November 02, 2013

Citation: Tan JW, Zhang CR, Huang FF (2013) Ocular Phenotypes and *In Vivo* Laser Confocal Microscopy Findings in a Family with Schnyder Corneal Dystrophy Shared the Same *UBIAD1* Mutation Locus (N102S). J Clin Exp Ophthalmol 4: 303. doi: 10.4172/2155-9570.1000303

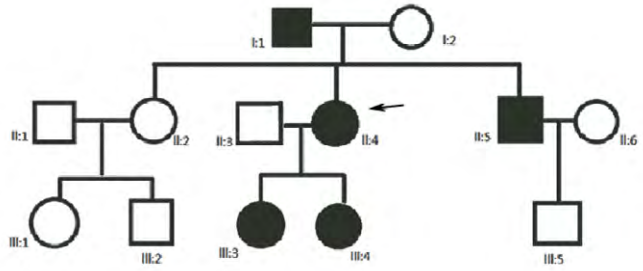

Figure 1: In the family tree, the black arrow indicates the proband.

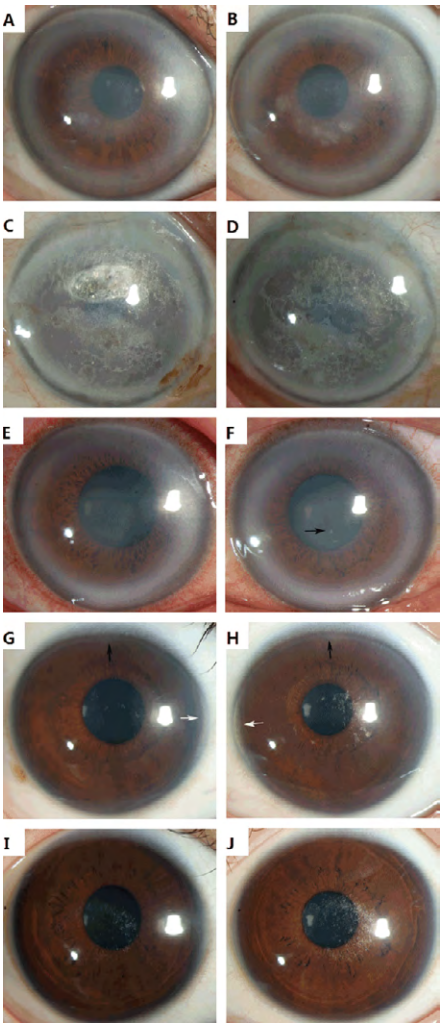

Figure 2: Slit-lamp photographs of five affected patients. The right pictures indicate the left eye and the left pictures indicate the right eye. (A and B): Case 1. (C and D): Case 2. (E and F): Case 3, no crystals were found in the right eye, but with crystals in the left eye (black arrows). (G and H): Case 4, crescent-shaped opacifications (white arrows) and incomplete arcus lipoides (black arrows) were observed in the limbus of both corneas. (I and J): Case 5.

generation Chinese family (Figure 1). The proband (case 1, II: 4), a 46-year-old woman presented with a three-year history of white rings in her eyes. Her best-corrected visual acuity (BCVA) was 20/25 OU. Slit-lamp examination demonstrated that both corneas contained sheet and punctiform subepithelial crystalline materials, and central disciform opacity with arcus lipoides (Figures 2A and 2B). The proband's father (case 2, I: 1), a 68-year-old man, presented with gradual bilateral painless reduction of vision over the past 30 years, and complained of glares and a marked decrease in vision in bright light. His BCVA was HMGP (hand movement with good projection) OU in bright environment, and 20/50 OD, 20/70 OS in dark environment. Slit-lamp examination revealed numerous subepithelial crystalline deposits, diffuse corneal opacities and remarkable arcus lipoides bilaterally (Figures 2C and 2D). The proband's brother (case 3, II: 5), a 40-year-old man, whose BCVA was 20/25 OU had no ocular discomfort. Bilateral slit-lamp examination also demonstrated central stromal disciform opacity and arcus lipoides in the corneas. No crystals were found in the right eye (Figure 2E), but some punctiform subepithelial crystals were observed in the left eye (Figure 2F). The proband's older daughter (case 4, III: 3), a 16-year-old girl without ocular discomfort. Her UCVA was 20/20 OU. Ophthalmic examination revealed a central subepithelial crystal, incomplete arcus lipoides and crescent-shaped opacifications which appeared to be bilaterally symmetrical (Figures 2G and 2H). The proband's younger daughter (case 5, III: 4), a 8-year-old girl also had no ophthalmic complaints. Her BCVA was 20/20 OU. Ophthalmic examination showed central annular crystals in both corneas (Figures 2I and 2J).

In vivo laser confocal microscopy

The proband (case 1, II: 4), IVCM of both corneas revealed that the basal epithelial layer appeared normal. A number of translucent basal/subepithelial nerves were identified in the Bowman layer (Figure 3A). In the anterior and mid stroma, more highly reflective, short rod-like crystalline materials were found (Figures 3B and 3C). In the posterior stroma, crack-like striaes were observed (Figure 3D). The endothelium was undetectable because of the large, highly reflecting crystalline deposits in the anterior stroma.

The proband's father (case 2, I: 1), IVCM of both corneas identified brightly reflective flake-shaped materials in the basal epithelium (Figure 4A). The basal epithelial/subepithelial nerve plexus cannot be observed. Brightly reflective crystalline materials could be shown in the stroma, and the crystals were long needle or block shaped (Figure 4B). The endothelial cell layer could not be visualized properly.

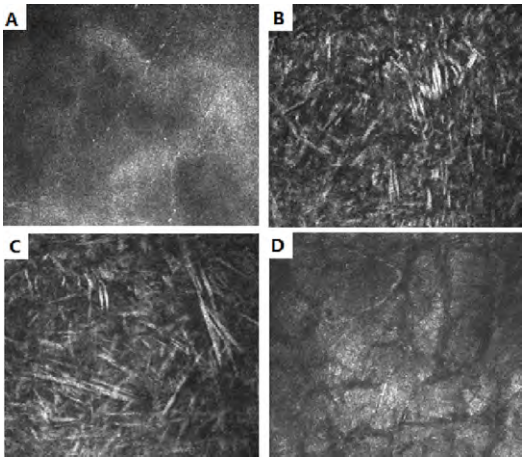

Figure 3: (A) *In vivo* laser confocal microscopic images of the translucent basal/subepithelial nerves. (B and C) Brightly reflective crystalline materials were found in the anterior and mid stroma. (D) Crack-like striaes were observed in the posterior stroma.

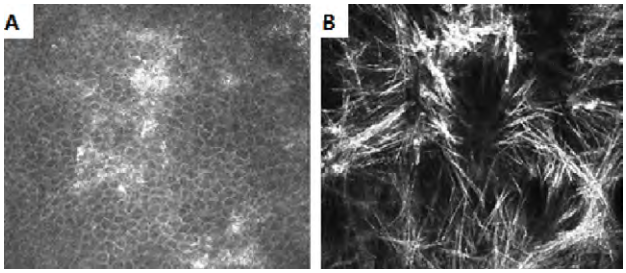

Figure 4: (A) *In vivo* laser confocal microscopic images of corneal lesions, brightly reflective flake-like materials were found in the basal epithelium. (B) Brightly reflective needle-shaped crystalline depositions were observed in the stroma.

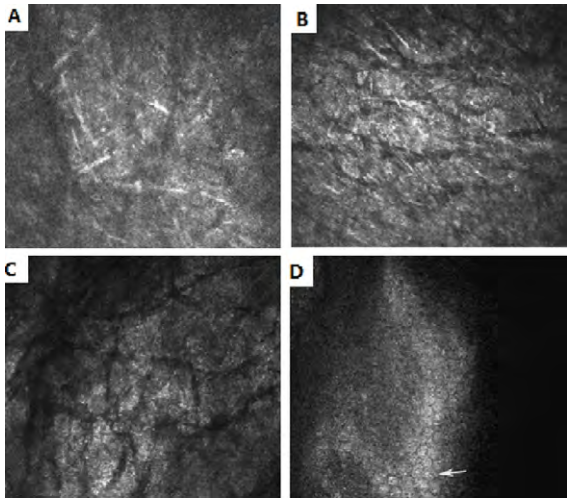

Figure 5: (A) *In vivo* laser confocal microscopic images identified brightly reflective crystalline materials were found in the anterior stroma. (B and C) Crack-like striaes were showed in the mid and posterior stroma. (D) Highly reflective dots were observed into endothelial cells (black arrow).

The proband's brother (case 3, II: 5), IVCM of both corneas revealed that the basal epithelial cell layer was normal. In the anterior stroma, a small number of highly reflective, short rod-like crystalline materials were shown (Figure 5A). Also, crack-like striaes upward to the anterior stromal layer and downward to the posterior stromal layer were identified (Figures 5B and 5C). Endothelial cells appeared to contain highly reflective intracellular deposits (Figure 5D).

Molecular genetic analysis

Genotyping indicated linkage to the locus at chromosome 1p36, and a direct sequencing analysis of *UBIAD1* in this family identified a heterozygous point mutation at position c. 305A>G within exon 1. This mutation led to a conversion from asparagine at position 102 to serine (N102S) in five affected patients but not in the unaffected individuals (Figure 6).

Discussion

In our study, all of the affected individuals had a predictable pattern of corneal opacity which was dependent on age, except for cases 4 and 5. According to a study published previously [4], patients under the age of 23 years showed only a central corneal opacity, which may involve the entire stroma with or without central crystalline deposits. Patients aged 23-39 years showed arcus lipoides, and these older than 39 years had mid-peripheral haze. In the absence of central corneal opacity, case 4 showed incomplete arcus lipoides. Furthermore, cases 4 and 5 presented subepithelial crystalline deposits, but without central corneal opacity. This suggests that the classification of corneal opacity by age was inconclusive, even though a sequential developmental pattern could be observed. Varied shapes (punctate, sheet or annular corneal crystalline depositions) were noted in different individuals of different ages. A similar phenotype was demonstrated in a pedigree of (cases 1 and 3) and (cases 4 and 5) by slit-lamp photographs, respectively. In contrast, the pedigree of second (cases 1 and 3) and third generation (cases 4 and 5) descendents presented a significantly different phenotypes of SCD. The second generation (cases 1 and 3) presented mildly punctiform and sheet crystals in the corneal subepithelium with central disciform opacities; however, the third generation (cases 4 and 5) had a severely circular pattern of crystalline deposits in the corneal subepithelium. Phenotypes of SCD patients in different generations seemed to be significantly different. These conclusions could not be ascertained, but similar findings also appeared in other SCD families as some previous studies reported [5-8].

Meanwhile, we examined three adult patients (cases 1, 2 and 3) under IVCM. Examination of case 2 showed highly reflective flake-shaped materials in the basal epithelial layer. A few of translucent basal/subepithelial nerves were observed in case 1. According to previous studies, both light and electron microscope examinations showed lipid or cholesterol deposits on the basal epithelial cell layer, Bowman's membrane layer, stromal layer, and occasionally in the corneal endothelial cell layer [3,9-11]. Minna et al. have reported that local defect of lipid metabolism is present in corneal cells in SCD, which lead to lipid deposits inside and around the cell at the early stage. Later, the extracellular deposits become larger [10]. Therefore, the highly reflective flake-shaped material on the basal epithelial layer could be abnormal lipid or cholesterol accumulations. The epithelial/subepithelial innervation could be damaged, due to increasing lipid or cholesterol accumulations [10]. Massive highly reflective needle-shaped materials appeared in stroma on case 2, yet cases 1 and 3 had highly reflective short rod-like materials. An interesting finding was the occurrence of the crack-like striaes, which were observed in the stroma of cases 1 and 3. The precise origin of the crack-like striaes have not been identified or reported. Some highly reflective dot deposits were found inside the endothelial cell in case 3. Based on Minna et al. study [10], these highly reflective dots could be lipid or cholesterol deposits.

In case 3, only the left eye had crystalline deposits under slit-lamp examination. However, deposits of short rod-like crystalline materials could be found in the anterior stroma in both corneas under IVCM. So far, the diagnostic decision between crystalline and non-crystalline SCD has mainly relied on slit-lamp examination. In some cases, a small quantity of crystalline materials cannot be detected by slit-lamp examination. However, it may be detected later as the crystalline materials accumulate. Therefore, it is not reliable to diagnose non-crystal type SCD just based on the slit-lamp examinations. In clinical practice, only 54% of SCD patients have corneal crystals [3], and non-crystal type SCD may increase the difficulty of diagnosis. As a supplementary examination, ICVM can detect the existence of crystalline accumulations at cellular level, even if they could not be observed via slit-lamp examination. IVCM could decrease the difficulty of making the diagnosis of SCD.

In conclusion, further evaluations of the relationships between genotype and phenotype are required. As a non-invasive tool, IVCM is helpful in the diagnosis of SCD subtypes. Whether crack-like striaes

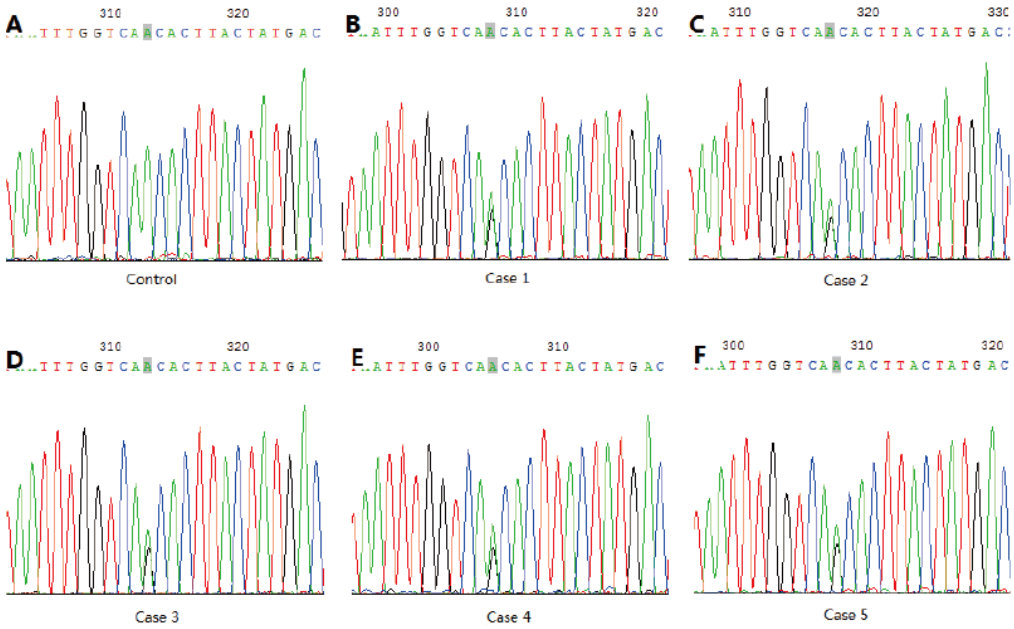

Figure 6: (A) Normal sequence of *UBIAD1* near codon 102 detected in an unaffected control is shown for comparison. (B-F) *UBAID1* sequencing revealed that the same heterozygous mutation (N102S) in exon 1, resulting from the AAC>AGC nucleotide substitution in five affected patients with SCD (Case 1, 2, 3, 4 and 5).

are the characteristic feature for our patients or an unavoidable stage during the development of SCD disease still requires further research.

Acknowledgment

The authors indicate no financial conflict of interest, and there was no financial support.

References

1. Yamada M, Mochizuki H, Kamata Y, Nakamura Y, Mashima Y (1998) Quantitative analysis of lipid deposits from Schnyder's corneal dystrophy. Br J Ophthalmol 82: 444-447.
2. Rodrigues MM, Kruth HS, Krachmer JH, Willis R (1987) Unesterified cholesterol in Schnyder's corneal crystalline dystrophy. Am J Ophthalmol 104: 157-163.
3. Weiss JS (2007) Visual morbidity in thirty-four families with Schnyder crystalline corneal dystrophy (an American Ophthalmological Society thesis). Trans Am Ophthalmol Soc 105: 616-648.
4. Weiss JS (2009) Schnyder corneal dystrophy. Curr Opin Ophthalmol 20: 292-298.
5. Du C, Li Y, Dai L, Gong L, Han C (2011) A mutation in the UBIAD1 gene in a Han Chinese family with Schnyder corneal dystrophy. Mol Vis 17: 2685-2692.
6. Mehta JS, Vithana EN, Venkataraman D, Venkatraman A, Yong VH, et al. (2009) Surgical management and genetic analysis of a Chinese family with the S171P mutation in the UBIAD1 gene, the gene for Schnyder corneal dystrophy. Br J Ophthalmol 93: 926-931.
7. Jing Y, Liu C, Xu J, Wang L (2009) A novel UBIAD1 mutation identified in a Chinese family with Schnyder crystalline corneal dystrophy. Mol Vis 15: 1463-1469.
8. Al-Ghadeer H, Mohamed JY, Khan AO (2011) Schnyder Corneal Dystrophy in a Saudi Arabian Family with Heterozygous UBIAD1 Mutation (p.L121F). Middle East Afr J Ophthalmol 18: 61-64.
9. Arnold-Wörner N, Goldblum D, Miserez AR, Flammer J, Meyer P (2012) Clinical and pathological features of a non-crystalline form of Schnyder corneal dystrophy. Graefes Arch Clin Exp Ophthalmol 250: 1241-1243.
10. Vesaluoma MH, Linna TU, Sankila EM, Weiss JS, Tervo TM (1999) In vivo confocal microscopy of a family with Schnyder crystalline corneal dystrophy. Ophthalmology 106: 944-951.
11. Weiss JS, Rodrigues MM, Kruth HS, Rajagopalan S, Rader DJ, et al. (1992) Panstromal Schnyder's corneal dystrophy. Ultrastructural and histochemical studies. Ophthalmology 99: 1072-1081.